Resonating-valence-bond ground state of lithium nanoclusters

D. Nissenbaum,[1] L. Spanu,[2,3] C. Attaccalite,[4] B. Barbiellini,[1] and A. Bansil[1]
[1]*Department of Physics, Northeastern University, Boston, Massachusetts 02115, USA*
[2]*INFM-Democritos, National Simulation Center and International School for Advanced Studies (SISSA), I-34014 Trieste, Italy*
[3]*Department of Chemistry, University of California at Davis, One Shield Avenue Davis, California 95616, USA*
[4]*Universidad del Pais Vasco, Unidad de Fisica de Materiales, San Sebastian, Spain E-20018*
(Received 3 October 2008; published 23 January 2009)

We have performed diffusion quantum Monte Carlo simulations of Li clusters showing that resonating-valence-bond (RVB) pairing correlations between electrons provide a substantial contribution to the cohesive energy. The RVB effects are identified in terms of electron transfers from *s*-like to *p*-like character, constituting a possible explanation for the breakdown of the Fermi-liquid picture observed in recent high-resolution Compton scattering experiments for bulk Li.

DOI: 10.1103/PhysRevB.79.035416 PACS number(s): 71.15.Nc, 31.15.xw, 02.70.Ss

Lithium, and other alkali metals, have been modeled as free-electron-like systems—an electron gas permeated by ions.[1] Nevertheless, in recent years, experimental and theoretical investigations of Li have revealed a more complex phase diagram.[2,3] Even at ambient pressure, the electron momentum density cannot be described adequately in terms of Fermi-liquid theory because pronounced deviations have been observed in bulk Li in recent high-resolution Compton scattering experiments.[4,5] Such deviations from the standard metallic picture can be ascribed to the possible existence of significant pairing correlations in the ground state.[6] Bonding properties have also revealed that Li behaves like a "bad" free-electron metal.[7]

The notion of stabilizing the metallic state through the creation of a resonant valence bond (RVB) state involving the metallic orbitals dates back to the early works of Pauling,[8] who first applied this picture to the Li ground state. In 1987, Anderson[9] proposed the RVB wave function as the natural ground state for the high-temperature superconducting materials, arguing that this picture is capable of capturing many aspects of the phase diagram of the cuprates.[10,11] More recently, it has been shown[12] that Pauling's RVB idea cannot account for all of the properties of metals that depend on the existence of a Fermi Surface (FS). However, since the nature of the FS in bulk Li has been questioned by the high-resolution Compton scattering studies,[5] it is natural to ask if the RVB paradigm might provide a viable model of the Li ground state.

This work demonstrates that RVB pairing correlations between electrons provide a contribution to the total energy of Li clusters of about 20 meV or greater per atom. The pairing correlation effects modify the electron momentum density distribution[6] and therefore provide a possible mechanism for the breakdown of the Fermi-liquid picture in bulk Li.

A number of authors have performed calculations on bulk Li as well as Li nanoclusters[7] but an implementation of the RVB model for Li clusters utilizing quantum Monte Carlo (QMC) simulations has not been attempted. A previous RVB study of small Li clusters[13] did not possess the accuracy of modern QMC methodologies. Here, we report QMC calculations of correlation effects beyond the limitations of the standard Jastrow-Slater (JS) wave function (WF) for the Fermi-liquid ground state[14] by employing the RVB. Specifically, we have used the Jastrow antisymmetrized geminal product (Jastrow+AGP, or JAGP), developed by Sorella and co-workers,[15–19] as a QMC variational ansatz for the RVB. We have performed diffusion Monte Carlo (DMC) calculations to obtain precise estimates of the energy, with this technique being limited in accuracy only by the nodal structure of the variational ansatz.[20,21] For a useful DMC study of bulk Li, see Ref. 22. For all our Li clusters, we obtain a distinct nodal structure improvement of the cohesive energy in comparison to standard JS WFs. An eigenvalue analysis of the pairing wave function further confirms the RVB nature of the ground state.

Our calculations employ the JAGP WF, defined as the product of a Jastrow term J and an antisymmetrized determinant Ψ_{AGP}: $\Psi_{\mathrm{JAGP}}(r_1,\ldots,r_N)=\Psi_{\mathrm{AGP}}(r_1,\ldots,r_N)J(r_1,\ldots,r_N)$. The determinant Ψ_{AGP} is constructed as $\Psi_{\mathrm{AGP}}=\hat{A}[\Phi(r_1^{\uparrow},r_1^{\downarrow})\cdots\Phi(r_{N/2}^{\uparrow},r_{N/2}^{\downarrow})]$, where $\hat{A}$ is the antisymmetrization operator, $\Phi(r_1^{\uparrow},r_1^{\downarrow})$ is the pairing function, and N is the number of electrons in the system (N must be even for this formulation; see Ref. 23 for an extension to open-shell systems). The pairing function Φ is defined as $\Phi(r^{\uparrow},r^{\downarrow})=\psi(r^{\uparrow},r^{\downarrow})1/\sqrt{2}(|\uparrow\downarrow\rangle-|\downarrow\uparrow\rangle)$, where the spin part is a singlet. The spatial part ψ—the geminal—is represented by a pairing expansion over a local single-particle basis set $\{\phi_i\}$, i.e.,

$$\psi(r^{\uparrow},r^{\downarrow})=\sum_{i,j}\lambda_{i,j}\phi_i(r^{\uparrow})\phi_j(r^{\downarrow}). \tag{1}$$

Here, indices i and j run over different orbitals (covering all nuclear sites), which are expanded in a Gaussian basis set centered on the nuclear positions.[24] The Jastrow factor $J=J_1J_2J_3$ is composed of an electron-nuclear (J_1), an electron-electron (J_2), and an electron-electron-nuclear (J_3) term; it guarantees that the cusp conditions are satisfied and it allows the correct charge distribution in the system. The J_3 term is constructed in a form similar to the pairing function of Eq. (1).[16] The Jastrow parameters, λ parameters, Gaussian (Slater) orbital exponents, and orbital coefficients have been optimized by energy minimization using the methods described in Refs. 20 and 25.

We have compared the JAGP wave function with three types of single-determinant JS wave functions: one involving

TABLE I. DMC all-electron calculations comparing the JS-HF and the JAGP wave function for Li clusters. The first two columns present the total energy/atom. The next two columns show the cohesive energy/atom, and the final column is the difference between these two cohesive energies.

N	$E_{\mathrm{DMC}}^{\mathrm{JS\text{-}HF}}$ (hartree)	$E_{\mathrm{DMC}}^{\mathrm{JAGP}}$ (hartree)	$E_{\mathrm{coh}}^{\mathrm{JS\text{-}HF}}$ (eV)	$E_{\mathrm{coh}}^{\mathrm{JAGP}}$ (eV)	ΔE_{coh} (meV)
2	−7.495 93(8)	−7.4971(1)	0.491(2)	0.522(3)	32(5)
4	−7.5036(1)	−7.504 85(13)	0.699(3)	0.733(4)	34(6)
8	−7.5130(1)	−7.514 40(23)	0.955(3)	0.993(6)	38(9)

a standard Slater determinant of Hartree-Fock (HF) orbitals (abbreviated as JS-HF), one utilizing a pseudopotential to replace the core electrons and utilizing Kohn-Sham orbitals for the valence electrons calculated within the density functional theory (DFT) using the local density approximation (LDA) (abbreviated as JS-LDA), and a wave function defined as the limiting case of the JAGP wave function in which the occupation of the virtual orbitals is forced to be zero (JS-V0). The latter wave function possesses the standard JS form. The geometries of all our Li clusters were optimized using the software JAGUAR with a 63111G basis set and the B3LYP exchange-correlation potential.[26,27]

For the all-electron JS-HF wave function, we examined clusters of two, four, and eight Li atoms modeled with HF orbitals obtained from the software JAGUAR.[26] The wave function included the J_1 and J_2 terms, which were optimized using an improved version of the stochastic gradient approximation (SGA) (Ref. 28) method. Our corresponding DMC results are given in Table I for the dimer, the planar cluster Li_4, and the three-dimensional Li_8. For all three clusters, we obtain distinct corrections of about 30 meV/atom for the cohesive energy. Figure 1 illustrates the results. The DMC values with the JS wave functions are already quite good because the cohesive energy, E_{coh}, compares fairly well with the experimental values given in Ref. 29, and because JS DMC calculations are known to retrieve better than 90% of the correlation energy.[30] Also, in both cases we observe the expected increase in cohesive energy with cluster size, describing the tendency for these clusters to grow.[29] However, the inset of Fig. 1 shows that the difference $\Delta E = E_{\mathrm{coh}}^{\mathrm{JAGP}} - E_{\mathrm{coh}}^{\mathrm{JS\text{-}HF}}$, i.e., the nodal structure corrections, are about 30 meV/atom.

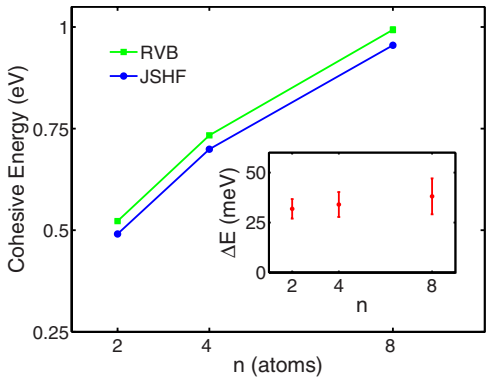

FIG. 1. (Color online) Cohesive energies per atom for Li_n with $n=2$, 4, and 8, representing systems of dimension $d=1$, 2, and 3, respectively, calculated using the diffusion quantum Monte Carlo all-electron method. The plot compares the RVB nodal structure against the standard HF nodal structure. The error bars are comparable to the size of the points and lines connect points to guide the eye. The inset shows the difference in cohesive energies between the models.

The bonding properties of Li can be described quite accurately by replacing the core electrons with a pseudopotential because the 1*s* core states do not contribute significantly to bonding. For example, pseudopotential DMC calculations successfully predict the small binding energy for the LiPs molecule,[31] in accordance with the results of more sophisticated DMC all-electron calculations.[32] Another advantage of the pseudopotential is the possibility of relatively straightforwardly disentangling the valence characteristics of the $\Lambda = \lambda_{ij}$ matrix in Eq. (1) from core contributions. This submatrix will also be seen below to help identify an RVB signature in the wave function.

We consider the JS-LDA pseudopotential wave function for Li clusters containing 2, 4, 8, and 20 atoms in order to assess the impact of these one-body orbitals on the nodal structure. The inner 1*s* core electrons were replaced by the norm-conserving pseudopotential provided by Burkatzki *et al.*[33] The wave function was constructed using Kohn-Sham LDA orbitals obtained with the PWSCF code.[34] The LDA calculations used a cubic simulation cell of 40 a.u. sides, a plane-wave cutoff of 70 Ry, and included optimized J_1 and J_2 terms. A modified version of the DMC, the lattice regularized diffusion Monte Carlo (LRDMC) (Ref. 35) method, was used, which allows the inclusion of a nonlocal pseudopotential in a consistent variational scheme. The JS-LDA DMC results are summarized in Table II. In this case also, the JAGP yields the lowest total energies. These results confirm that in the case of Li clusters the RVB nodal structure provides a correction to the cohesive energy, which tends to be more than 20 meV/atom.

The signature of an RVB state can be directly identified by analyzing the eigenvalues and eigenvectors of the matrix $\Lambda = \lambda_{ij}$ in Eq. (1). Given the Λ matrix, we solve the eigenvalue problem $\Lambda S\vec{u} = \mu\vec{u}$, where S is the overlap matrix between the local basis set orbitals, i.e., $S_{ij} = \langle \phi_i \phi_j \rangle$, and $\vec{u}$ are the eigenvectors representing the basis of natural orbitals, with corresponding eigenvalues providing the geminal coefficients associated with the occupation numbers.[36] Anderson[9] has shown that a signature of the RVB state is given by a change in sign of the eigenvalues μ when passing from occupied to virtual states with a significant weight for the virtual states. This trend also helps to reduce double occupancy

TABLE II. Same as Table I, except here DMC pseudopotential calculations are used to compare the JS-LDA and the JAGP wave function. This data set includes Li_{20}.

N	$E_{DMC}^{JS\text{-}LDA}$ (hartree)	E_{DMC}^{JAGP} (hartree)	$E_{coh}^{JS\text{-}LDA}$ (eV)	E_{coh}^{JAGP} (eV)	ΔE_{coh} (meV)
2	−0.213 18(4)	−0.215 34(8)	0.459 32(7)	0.516 25(9)	56.9(2)
4	−0.221 00(3)	−0.223 57(5)	0.672 12(6)	0.740 20(6)	68.1(1)
8	−0.231 52(3)	−0.232 25(1)	0.958 39(6)	0.976 40(2)	18.01(8)
20	−0.237 750(5)	−0.238 93(1)	1.127 91(4)	1.158 17(2)	30.26(6)

at lattice sites, as in the Heitler London limit.

This diagonalization was performed for Li_4, Li_8, and Li_{20} with pseudopotential. Figure 2 shows the eigenvalues. Positive eigenvalues are in the top portion of the figure, while the negative eigenvalues are shown in the bottom on an expanded scale. The presence of the RVB signature indicates a departure from the standard JS nodal structure, and by extension into the bulk, a departure from the Fermi-liquid picture.[14] This departure can be explained as follows. If the generating geminal yields a standard JS ansatz, the occupied orbitals would have equal weights, and the remaining orbitals would not contribute. However, in the case of the RVB, the virtual orbitals have significant nonzero amplitudes but with opposite sign. Contrary to the standard JS description, virtual orbitals, i.e., orbitals with index greater than $N/2$, have a small but finite negative eigenvalue, which is related to the occupancy.

The behavior of the eigenvalues in Fig. 2 confirms the fact that the AGP structure of the Li dimer studied by Elander *et al.*[37] for various atomic separations captures general features which suggest a certain robustness of the RVB signature with respect to the exact geometry of Li clusters. It is interesting to note that the natural orbitals corresponding to the leading eigenvalues contain a significant p character. An important $2p-2p$ π contribution was observed in the AGP wave function for Li_2,[37] causing a departure from the standard JS nodal structure. Recent experiments found that Li impurities in an Al matrix produce an anomalous transfer

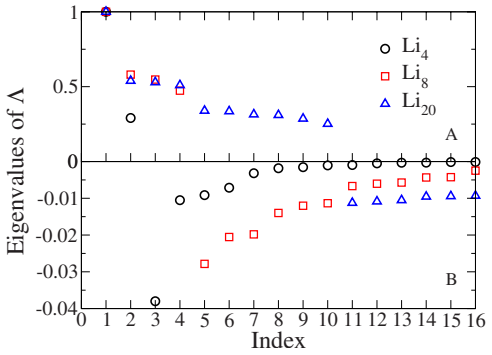

FIG. 2. (Color online) Eigenvalues of the diagonalized Λ matrix, representing the occupation of the natural geminal orbitals. Top half: eigenvalues for the first $\frac{N}{2}$ natural orbitals. Bottom half: expanded view of the eigenvalues for the virtual orbitals. Unlike a standard Jastrow-Slater wave function, the JAGP allows occupancy of the higher-level orbitals. A characteristic of the RVB is a sign flip when passing from the primary to the virtual orbitals.

from s-like to p-like character, and thus constitute another example in which the standard Fermi-liquid picture breaks down and properties of the correlated inhomogeneous electron gas must be considered.[38]

Table III provides the results of variational Monte Carlo (VMC) calculations, rather than DMC, of the JS-LDA and the JAGP wave functions, confirming the relatively high quality of the JAGP wave function at the variational level. A comparison of Tables II and III indicates that our variational results using the JAGP are superior to the diffusion results using the JS-LDA for Li_2 and Li_4. Table III also shows the significantly smaller variance of the local energy for the RVB wave function, indicating more efficient and less time-consuming calculations,[27] as well as a wave function that may be approaching the exact solution. Interestingly, for the Li_2 molecule the JAGP is able to recover 95.7% and 99.45% of the correlation energy[16] at the VMC and DMC levels, respectively, while the corresponding values with backflow corrections[39] are 87.79% and 97.1%. Therefore, in the present case, the RVB correlations appear to dominate other effects. Moreover, the possibility that the RVB Pauling structures provide an important contribution in the configuration-interaction (CI) expansion has also been suggested in a recent quantum chemical study for the neutral Li_4 cluster.[40]

Finally, to directly measure nodal structure effects, we have utilized the limiting JS-V0 wave function. In this way, we can estimate the energy contribution from occupation of the virtual orbitals by forcing the pairing wave function to possess only the $N/2$ fully occupied orbitals with zero occupancy of the virtual orbitals. These calculations were performed for Li_4, Li_8, and Li_{20} with pseudopotential, and in all

TABLE III. VMC calculations of the JS-LDA and the JAGP wave function for Li clusters. The first two columns compare the total energy/atom. The variational JAGP results for Li_2 and Li_4 are lower than the diffusion JS-LDA results from Table II, indicating superior performance of the wave function even at the variational level for the JAGP than can be obtained at the diffusion level for the JS-LDA. The final two columns show the variance σ^2 of the local energy/atom. The JAGP shows a smaller variance than the JS-LDA.

N	$E_{VMC}^{JS\text{-}LDA}$ (hartree)	E_{VMC}^{JAGP} (hartree)	$\sigma^2_{JS\text{-}LDA}$ (eV)	σ^2_{JAGP} (eV)
2	−0.205 61(4)	−0.215 09(3)	0.2921(9)	0.068(5)
4	−0.208 99(4)	−0.222 59(2)	0.392(3)	0.0477(9)
8	−0.216 16(2)	−0.231 200(6)	0.388(3)	0.0662(5)
20	−0.218 34(2)	−0.2371(1)	0.602(2)	0.011(1)

three cases, VMC as well as DMC calculations find an improvement of at least 20 meV/atom in the cohesive energy due to the RVB nodal structure, consistent with the DMC results of Table II. As stated previously, the definition of JS-V0 assures that the Jastrow factor, basis set, and functional form are identical in the JAGP and in the JS-V0 wave functions so that $\Delta E_{\mathrm{RVB}}=E_{\mathrm{coh}}^{\mathrm{JAGP}}-E_{\mathrm{coh}}^{\mathrm{JS\text{-}V0}}$ is a direct calculation of the resonance energy. This confirms that the gain in energy is a consequence of the RVB orbitals, and not the result of a different Jastrow factor or a different single-particle basis set.

In conclusion, we have performed DMC calculations of Li clusters with an RVB guiding WF, utilizing a fundamentally different nodal structure than the standard JS WF. We find that the RVB nodal structure is able to recover about 20 meV of cohesive energy/atom. Furthermore, we have identified a distinct RVB signature in an eigenvalue decomposition of the JAGP Λ matrix, suggesting modifications of the electron occupation numbers due to RVB effects. These results justify use of an approximation for AGP correlation effects in momentum density calculations[6] and might explain deviations from the Fermi-liquid picture observed in recent high-resolution Compton scattering experiments on bulk Li.

We acknowledge useful discussions with R. S. Markiewicz. This work was supported by the Division of Materials Science and Engineering, Basic Energy Sciences, Office of Science of the U.S. Department of Energy, Contract No. DE-FG02-07ER46352, and benefited from the allocation of supercomputer time at the NERSC and the Northeastern University's Advanced Scientific Computation Center (NU-ASCC). The work was also supported by the U.S. Department of Energy, Scidac, Contract No. DE-FC02-06ER25794.

[1] N. W. Ashcroft and N. D. Mermin, *Solid State Physics* (Saunders College, Philadelphia, 1976).
[2] J. B. Neaton and N. W. Ashcroft, Nature (London) **400**, 141 (1999).
[3] M. Hanfland, K. Syassen, N. E. Christensen, and D. L. Novikov, Nature (London) **408**, 174 (2000).
[4] Y. Sakurai, Y. Tanaka, A. Bansil, S. Kaprzyk, A. T. Stewart, Y. Nagashima, T. Hyodo, S. Nanao, H. Kawata, and N. Shiotani, Phys. Rev. Lett. **74**, 2252 (1995).
[5] W. Schülke, G. Stutz, F. Wohlert, and A. Kaprolat, Phys. Rev. B **54**, 14381 (1996).
[6] B. Barbiellini and A. Bansil, J. Phys. Chem. Solids **62**, 2181 (2001).
[7] R. Rousseau and D. Marx, Chem.-Eur. J. **6**, 2982 (2000).
[8] L. Pauling, Nature (London) **161**, 1019 (1948).
[9] P. W. Anderson, Science **235**, 1196 (1987).
[10] P. A. Lee, N. Nagaosa, and X. G. Wen, Rev. Mod. Phys. **78**, 17 (2006).
[11] L. Spanu, M. Lugas, F. Becca, and S. Sorella, Phys. Rev. B **77**, 024510 (2008).
[12] P. Anderson, Phys. Today **61** (4) 8 (2008).
[13] J. R. Mohallem, R. O. Vianna, A. D. Quintão, A. C. Pavão, and R. McWeeny, Z. Phys. D: At., Mol. Clusters **42**, 135 (1997).
[14] P. Fulde, *Electron Correlations in Molecules and Solids* (Springer, Berlin, 1995).
[15] M. Casula and S. Sorella, J. Chem. Phys. **119**, 6500 (2003).
[16] M. Casula, C. Attaccalite, and S. Sorella, J. Chem. Phys. **121**, 7110 (2004).
[17] S. Sorella, M. Casula, and D. Rocca, J. Chem. Phys. **127**, 014105 (2007).
[18] C. Attaccalite and S. Sorella, Phys. Rev. Lett. **100**, 114501 (2008).
[19] F. Sterpone, L. Spanu, L. Ferraro, S. Sorella, and L. Guidoni, J. Chem. Theory Comput. **4**, 1428 (2008).
[20] C. J. Umrigar, J. Toulouse, C. Filippi, S. Sorella, and R. G. Hennig, Phys. Rev. Lett. **98**, 110201 (2007).
[21] L. Mitas, Phys. Rev. Lett. **96**, 240402 (2006).
[22] C. Filippi and D. M. Ceperley, Phys. Rev. B **59**, 7907 (1999).
[23] A. J. Coleman, J. Math. Phys. **13**, 214 (1972).
[24] For the all-electron case we use a Gaussian basis set of $8s6p$ contracted to $[3s1p]$, while in the psedopotential calculations a $4s4p$ contracts to $[2s1p]$.
[25] S. Sorella, Phys. Rev. B **71**, 241103(R) (2005).
[26] URL: http://www.schrodinger.com.
[27] D. Nissenbaum, B. Barbiellini, and A. Bansil, Phys. Rev. B **76**, 033412 (2007).
[28] A. Harju, B. Barbiellini, S. Siljamaki, R. M. Nieminen, and G. Ortiz, Phys. Rev. Lett. **79**, 1173 (1997).
[29] R. O. Jones, A. I. Lichtenstein, and J. Hutter, J. Chem. Phys. **106**, 4566 (1997).
[30] W. M. C. Foulkes, L. Mitas, R. J. Needs, and G. Rajagopal, Rev. Mod. Phys. **73**, 33 (2001).
[31] A. Harju, B. Barbiellini, S. Siljamaki, R. M. Nieminen, and G. Ortiz, J. Radioanal. Nucl. Chem. **211**, 193 (1996).
[32] D. Bressanini, M. Mella, and G. Morosi, J. Chem. Phys. **108**, 4756 (1998).
[33] M. Burkatzki, C. Filippi, and M. Dolg, J. Chem. Phys. **126**, 234105 (2007).
[34] URL: http://www.pwscf.org.
[35] M. Casula, C. Filippi, and S. Sorella, Phys. Rev. Lett. **95**, 100201 (2005).
[36] B. Barbiellini, J. Phys. Chem. Solids **61**, 341 (2000).
[37] N. Elander, E. Sangfelt, H. Kurtz, and O. Goscinski, Int. J. Quantum Chem. **23**, 1047 (1983).
[38] J. Kwiatkowska, B. Barbiellini, S. Kaprzyk, A. Bansil, H. Kawata, and N. Shiotani, Phys. Rev. Lett. **96**, 186403 (2006).
[39] P. López Ríos, A. Ma, N. D. Drummond, M. D. Towler, and R. J. Needs, Phys. Rev. E **74**, 066701 (2006).
[40] A. D. Quintao and R. O. Vianna, Int. J. Quantum Chem. **81**, 76 (2001).